Proceedings of the ASME 2016 Pressure Vessels & Piping Conference
PVP 2016
July 17 - 21, 2016, Vancouver, BC, Canada

PVP2016-63539

A LAGRANGE-PROJECTION-LIKE NUMERICAL SCHEME FOR MIXED ACOUSTIC-CONVECTIVE TWO-PHASE FLOWS

Marco F.P. ten Eikelder*
Department of Mathematics and Computer Science
Eindhoven University of Technology
P.O. Box 513, 5600 MB Eindhoven
The Netherlands
Email: m.f.p.t.eikelder@tue.nl

Frédéric Daude
Analysis in Mechanics and Acoustics Department
Electricité de France R&D
1 avenue du Général de Gaulle
F-92140 Clamart
France
Email: frederic.daude@edf.fr

Barry Koren
Department of Mathematics and Computer Science
Eindhoven University of Technology
P.O. Box 513, 5600 MB Eindhoven
The Netherlands
Email: b.koren@tue.nl

ABSTRACT

The computation of compressible two-phase flows with the Kapila five-equation model is studied. In the model (fast) acoustic waves and (slow) transport waves occur. In this paper a splitting-based Lagrange-projection-like numerical scheme for the Kapila five-equation model is introduced to decouple these physical phenomena. This approach is based on a Lagrange-projection method for the gas dynamics equations. The decoupling leads to two submodels which are alternately solved to approximate the solution of the full model. The acoustic submodel is cast into an almost conservative form and is solved using an HLLC-type Riemann solver. A classical upwind scheme is used for the transport part. The method allows for a general equation of state. Numerical computations are performed for two-phase shock tube problems, including a mixture problem. The results are in good agreement with reference results.

Key words

two-phase flow; five-equation model; Lagrange-projection-scheme; shock-tube problems.

NOMENCLATURE

ρ	Bulk density.
u	Velocity.
p	Pressure.
e	Bulk internal energy density.
E	Bulk energy density.
c	Mixture speed of sound.
α_k	Volume fraction of the fluid k.
β_k	Mass fraction of the fluid k.
ρ_k	Density of fluid k.
e_k	Internal energy density of fluid k.
E_k	Energy density of fluid k.
c_k	Speed of sound of fluid k.
γ_k, π_k	Characteristic constants of fluid k.

*Address all correspondence to this author.

INTRODUCTION

Two-phase compressible flow phenomena arise in many natural features and industrial applications. Examples are oil-slick flows at sea, water-air flows in ship hydrodynamics, shock-bubble-interaction flows, etc. Furthermore, the study of two-phase flow is a challenging research area. Therefore, this topic is of interest to both engineers and researchers.

In this paper the five-equation model, which models inviscid, non-heat-conducting, compressible two-fluid flow, is considered. It allows a mixture of the two fluids. The original five-equation two-phase flow model of Kapila et al. [1] is derived from the two-fluid flow model of Baer and Nunziato [2]. Murrone and Guillard [3] give an analysis of the five-equation model and indicate that the reduced five-equation model is a good approximation of the seven equation two-fluid model. Kreeft and Koren [4] propose a new formulation of the five-equation model, in which the topological equation is replaced by an energy equation. An Osher-type approximation is used for the discretized system. Daude et al. [5] present computations with the original five-equation model of Kapila et al. [1] using an HLLC-type scheme in the context of Arbitrary Lagrangian-Eulerian formulation. Due to its simplicity, the original five-equation model of Kapila et al. [1] is considered.

A Lagrange-projection scheme has been developed for the Euler equations of gas dynamics by Chalons et al. [6]. In our paper their approach is extended to the full two-phase five-equation model.

In the first section the mathematical model is presented. The second section is devoted to a detailed description of the new numerical scheme, which is in turn assessed in the third section. Conclusions are given in the last section.

MATHEMATICAL MODEL

The dynamics of inviscid two-phase flow can be described by the five-equation model, which is a set of quasilinear hyperbolic partial differential equations. It consists of four balance equations for conservative quantities, which are the bulk mass, the bulk momentum, the bulk energy, and the mass of one of the two phases. The fifth equation is a topological equation which describes the evolution of the volume fraction.

Governing equations

The five-equation two-phase flow model of Kapila et al. [1] is considered:

$$\begin{aligned}
&\partial_t \rho && +\nabla\cdot(\rho\mathbf{u}) && && = 0, && \text{(1a)}\\
&\partial_t(\rho\mathbf{u}) && +\nabla\cdot(\rho\mathbf{u}\otimes\mathbf{u}) && +\nabla p && = \mathbf{0}, && \text{(1b)}\\
&\partial_t(\rho E) && +\nabla\cdot(\rho E\mathbf{u}) && +\nabla\cdot(p\mathbf{u}) && = 0, && \text{(1c)}\\
&\partial_t(\alpha_1\rho_1) && +\nabla\cdot(\alpha_1\rho_1\mathbf{u}) && && = 0, && \text{(1d)}\\
&\partial_t\alpha_1 && +\mathbf{u}\cdot\nabla\alpha_1 && +\phi\nabla\cdot\mathbf{u} && = 0, && \text{(1e)}
\end{aligned}$$

where t is the time parameter, ∇ denotes the gradient operator, ρ denotes the bulk density, $\mathbf{u}$ the velocity, p the pressure and E the bulk energy density. The variables α_k denote the volume fraction, with the saturation constraint $\alpha_1+\alpha_2=1$, and ρ_k the density of fluid k, respectively. In terms of single fluid variables, the bulk density and energy are given by

$$\rho = \alpha_1\rho_1 + \alpha_2\rho_2, \tag{2a}$$
$$\rho E = \alpha_1\rho_1 E_1 + \alpha_2\rho_2 E_2, \tag{2b}$$

where the energy densities of the fluids are

$$E_k = e_k + \frac{1}{2}\mathbf{u}\cdot\mathbf{u}, \tag{3}$$

with e_k the internal energy density of fluid k. The bulk internal energy density is given by

$$\rho e = \alpha_1\rho_1 e_1 + \alpha_2\rho_2 e_2, \tag{4}$$

and hence,

$$E = e + \frac{1}{2}\mathbf{u}\cdot\mathbf{u}. \tag{5}$$

Each phase is governed by an equation of state (EOS) $e_k = e_k(\rho_k, p)$, which allows the determination of the speed of sound of each single phase $c_k^2 = (p/\rho_k^2 - \partial_{\rho_k} e_k)(\partial_p e_k)^{-1}$. The interfacial variable in the topology equation (1e) is given by

$$\phi = \alpha_1\alpha_2\left(\frac{1}{\rho_2 c_2^2} - \frac{1}{\rho_1 c_1^2}\right) \Big/ \left(\frac{\alpha_1}{\rho_1 c_1^2} + \frac{\alpha_2}{\rho_2 c_2^2}\right). \tag{6}$$

To complete the model the stiffened gas (SG) equation of state (EOS) is used for both fluids, which reads as:

$$p = \rho_k e_k(\gamma_k - 1) - \gamma_k\pi_k, \tag{7}$$

where γ_k and π_k are characteristic constants of the thermodynamic behavior of fluid k. Using the SG EOS (7), the speed of sound of fluid k can be written as $c_k^2 = \gamma_k (p+\pi_k)/\rho_k$, and the bulk internal energy satisfies

$$\rho e = p\left(\frac{\alpha_1}{\gamma_1 - 1} + \frac{\alpha_2}{\gamma_2 - 1}\right) + \alpha_1 \frac{\gamma_1}{\gamma_1 - 1}\pi_1 + \alpha_2 \frac{\gamma_2}{\gamma_2 - 1}\pi_2. \quad (8)$$

Mathematical analysis

The five-equation model (1) can be cast, for the one-dimensional case, into the primitive form

$$\partial_t \mathbf{W} + \mathbf{B}(\mathbf{W})\partial_x \mathbf{W} = \mathbf{0}, \quad (9)$$

with

$$\mathbf{W} = \begin{pmatrix} \rho \\ u \\ p \\ \beta_1 \\ \alpha_1 \end{pmatrix}, \quad \mathbf{B}(\mathbf{W}) = \begin{pmatrix} u & \rho & 0 & 0 & 0 \\ 0 & u & 1/\rho & 0 & 0 \\ 0 & \rho c^2 & u & 0 & 0 \\ 0 & 0 & 0 & u & 0 \\ 0 & \phi & 0 & 0 & u \end{pmatrix}, \quad (10)$$

where $\beta_k = \alpha_k \rho_k / \rho$ denotes the mass fraction. Note that the first three equations, describing the bulk fluid, correspond to the Euler equations of gas dynamics. The derivation of the primitive equations (9)-(10) is straightforward and can be found in Kreeft and Koren [4]. The vector $\mathbf{W}$ contains the primitive variables. The eigenvalues of $\mathbf{B}(\mathbf{W})$ are:

$$\lambda_1 = u - c, \;\; \lambda_{2,3,4} = u, \;\; \lambda_5 = u + c. \quad (11)$$

The celerity, denoted by c, obeys the Wood formula [7]:

$$\frac{1}{\rho c^2} = \frac{\alpha_1}{\rho_1 c_1^2} + \frac{\alpha_2}{\rho_2 c_2^2}, \quad (12)$$

which corresponds to the mixture speed of sound. The characteristic fields associated with eigenvalues $\lambda_{2,3,4}$ are linearly degenerate (LD) and the other two fields are genuinely nonlinear (GNL) [3].

NUMERICAL SCHEME

A novel splitting-based Lagrange-projection-like numerical scheme is presented. First the splitting of the five-equation model is presented. Next, the treatment of the acoustic model is discussed for which a simple and robust HLLC-type Riemann solver is used. Finally, the upwind scheme for the transport submodel is given.

The splitting approach

The five-equation model deals with two kinds of wave speeds associated with its eigenvalues, i.e. the GNL waves are linked to pressure waves whereas the LD wave is connected to the material velocity. In certain situations, such as subsonic flows, the ratio between these two velocities can be large leading to inaccuracy with the use of approximate Godunov approaches. In order to decouple acoustic and transport phenomena, a splitting operator is proposed. This splitting is inspired by the splitting of the acoustic and transport waves for the Euler equations of gas dynamics proposed in [6].

By using chain rule arguments the five-equation model (1) is split into (i) the acoustic system:

$$\begin{aligned}
&\partial_t \rho && + \rho \nabla \cdot \mathbf{u} && && = 0, && (13a)\\
&\partial_t (\rho \mathbf{u}) && + \rho \mathbf{u} \nabla \cdot \mathbf{u} && + \nabla p && = \mathbf{0}, && (13b)\\
&\partial_t (\rho E) && + \rho E \nabla \cdot \mathbf{u} && + \nabla \cdot (p\mathbf{u}) && = 0, && (13c)\\
&\partial_t (\alpha_1 \rho_1) && + \alpha_1 \rho_1 \nabla \cdot \mathbf{u} && && = 0, && (13d)\\
&\partial_t \alpha_1 && + \phi \nabla \cdot \mathbf{u} && && = 0, && (13e)
\end{aligned}$$

and (ii) the transport system:

$$\begin{aligned}
&\partial_t \rho && + \mathbf{u} \cdot \nabla \rho && = 0, && (14a)\\
&\partial_t (\rho \mathbf{u}) && + \mathbf{u} \cdot \nabla (\rho \mathbf{u}) && = \mathbf{0}, && (14b)\\
&\partial_t (\rho E) && + \mathbf{u} \cdot \nabla (\rho E) && = 0, && (14c)\\
&\partial_t (\alpha_1 \rho_1) && + \mathbf{u} \cdot \nabla (\alpha_1 \rho_1) && = 0, && (14d)\\
&\partial_t \alpha_1 && + \mathbf{u} \cdot \nabla \alpha_1 && = 0. && (14e)
\end{aligned}$$

Note that the acoustic system contains all the pressure terms. Furthermore, the interfacial term of the topological equation is included in the acoustic system since it is a fast phenomenon (it includes the speed of sound).

The discretization of (1) consists of successively approximating the solution of the acoustic system and the transport system. By denoting the fluid state at time n with $\mathbf{Q}_j^n \equiv (\rho, \rho u, \rho E, \alpha_1 \rho_1, \alpha_1)_j^n$, and an intermediate time level with $n+1-$, the approximation of one time step reads:

1. Update $\mathbf{Q}_j^n$ to $\mathbf{Q}_j^{n+1-}$ approximating the solution of the acoustic system (13);
2. Update $\mathbf{Q}_j^{n+1-}$ to $\mathbf{Q}_j^{n+1}$ approximating the solution of the transport system (14).

Mathematical analysis splitting approach

The numerical simulations consist of one-dimensional problems, and therefore from now on, only the one-dimensional case is considered. The subsystems (13)-(14) can be cast into the

primitive forms: (i) for the acoustic subsystem:

$$\partial_t \mathbf{W} + \mathbf{A}(\mathbf{W})\partial_x \mathbf{W} = \mathbf{0}, \tag{15}$$

and (ii) for the transport subsystem:

$$\partial_t \mathbf{W} + \mathbf{T}(\mathbf{W})\partial_x \mathbf{W} = \mathbf{0}, \tag{16}$$

where

$$\mathbf{B}(\mathbf{W}) = \mathbf{A}(\mathbf{W}) + \mathbf{T}(\mathbf{W}), \tag{17}$$

with

$$\mathbf{A}(\mathbf{W}) = \begin{pmatrix} 0 & \rho & 0 & 0\,0 \\ 0 & 0 & 1/\rho & 0\,0 \\ 0 & \rho c^2 & 0 & 0\,0 \\ 0 & 0 & 0 & 0\,0 \\ 0 & \phi & 0 & 0\,0 \end{pmatrix}, \quad \mathbf{T}(\mathbf{W}) = u\,\mathbf{I}_5, \tag{18}$$

and $\mathbf{I}_d$ is the identity matrix in $\mathbb{R}^{d\times d}$. This casting reveals that the matrix $\mathbf{B}$ splits nicely into an acoustic part $\mathbf{A}$ and a transport part $\mathbf{T}$. The eigenvalues of the full system (λ_k) split into an acoustic part (a) and a transport part (t) as follows

$$\begin{aligned} &\lambda_1 = \lambda_1^a + \lambda_1^t,\ \lambda_{2,3,4} = \lambda_{2,3,4}^a + \lambda_{2,3,4}^t,\ \lambda_5 = \lambda_5^a + \lambda_5^t, \\ &\lambda_1^a = -c, \qquad \lambda_{2,3,4}^a = 0, \qquad \lambda_5^a = c, \\ &\lambda_1^t = u, \qquad \lambda_{2,3,4}^t = u, \qquad \lambda_5^t = u. \end{aligned} \tag{19}$$

The characteristic fields associated with the middle wave $\lambda_{2,3,4}^a = 0$ are linearly degenerate. The other two waves, associated with $\lambda_1^a = -c, \lambda_5^a = c$, can be shown, by using a similar argument as in [3], to be genuinely nonlinear in the non-isobaric case.

Acoustic subsystem

By taking $\{\tau, u, E, \beta_1, \alpha_1\}$ as set of variables, the acoustic system can be cast into the form

$$\begin{aligned} \partial_t \tau &- \tau\partial_x u &&= 0, && \text{(20a)} \\ \partial_t u &+ \tau\partial_x p &&= 0, && \text{(20b)} \\ \partial_t E &+ \tau\partial_x (pu) &&= 0, && \text{(20c)} \\ \partial_t \beta_1 & &&= 0, && \text{(20d)} \\ \partial_t \alpha_1 &+ \rho\phi\tau\partial_x u &&= 0. && \text{(20e)} \end{aligned}$$

Here $\tau = 1/\rho$ denotes the specific volume. Note that again the first three equations, Eq. (20a)-(20c), describe the bulk fluid, and the latter two, Eq. (20d)-(20e), describe the evolution of the fraction variables, which are specific for the five-equation two-phase flow model.

Note that the second term of each equation (except the fourth equation) contains the operator $\tau\partial_x$. By performing the change of variables $(x,t) \mapsto (m,t)$, where the mass variable m is defined by $m(x) := \int^x \rho(\tilde{x}, t^n)\mathrm{d}\tilde{x}$, this operator can be approximated by ∂_m. The Lagrangian system (up to an abuse of notation)

$$\begin{aligned} \partial_t \tau &- \partial_m u &&= 0, && \text{(21a)} \\ \partial_t u &+ \partial_m p &&= 0, && \text{(21b)} \\ \partial_t E &+ \partial_m (pu) &&= 0, && \text{(21c)} \\ \partial_t \beta_1 & &&= 0, && \text{(21d)} \\ \partial_t \alpha_1 &+ \rho\phi\partial_m u &&= 0, && \text{(21e)} \end{aligned}$$

is a first order in time approximation of (20). It can be written in vectorial form as

$$\partial_t \mathbf{Q}^{\mathrm{LAG}} + \partial_m \mathscr{F}^{\mathrm{LAG}}(\mathbf{Q}^{\mathrm{LAG}}) + \mathscr{R}^{\mathrm{LAG}}(\mathbf{Q}^{\mathrm{LAG}}, \partial_m \mathbf{Q}^{\mathrm{LAG}}) = \mathbf{0}, \tag{22}$$

where

$$\begin{aligned} \mathbf{Q}^{\mathrm{LAG}} &= (\tau, u, E, \beta_1, \alpha_1)^T, && \text{(23a)} \\ \mathscr{F}^{\mathrm{LAG}}(\mathbf{Q}^{\mathrm{LAG}}) &= (-u, p, pu, 0, 0)^T, && \text{(23b)} \\ \mathscr{R}^{\mathrm{LAG}}(\mathbf{Q}^{\mathrm{LAG}}, \partial_m \mathbf{Q}^{\mathrm{LAG}}) &= (0, 0, 0, 0, \rho\phi\partial_m u)^T. && \text{(23c)} \end{aligned}$$

The superscript LAG refers to *Lagrangian* variables. The term $\mathscr{F}^{\mathrm{LAG}}$ is a conservative flux and the term $\mathscr{R}^{\mathrm{LAG}}$ contains the non-conservative term.

HLLC-type solver for acoustic subsystem

An HLLC-type Riemann solver [8] is used to solve the acoustic subsystem. The finite-volume approximation of the acoustic system (22)-(23) on cell C_i reads

$$\begin{aligned} \partial_t((\mathbf{Q}^{\mathrm{LAG}})_i) + \frac{1}{\Delta m}\left((F^{\mathrm{LAG}})_{i+1/2}^{\mathrm{HLLC}} - (F^{\mathrm{LAG}})_{i-1/2}^{\mathrm{HLLC}}\right) \\ + \int_{C_i} \mathscr{B}\left((\mathbf{Q}^{\mathrm{LAG}})_i\right)\partial_m u \,\mathrm{d}V = 0, \end{aligned} \tag{24}$$

where the numerical flux F^{LAG} approximates $\mathscr{F}^{\mathrm{LAG}}((\mathbf{Q}^{\mathrm{LAG}}))$ and

$$\mathscr{R}^{\mathrm{LAG}}(\mathbf{Q}^{\mathrm{LAG}}, \partial_m \mathbf{Q}^{\mathrm{LAG}}) = \mathscr{B}\left(\mathbf{Q}^{\mathrm{LAG}}\right)\partial_m u, \tag{25}$$

with $\mathscr{B}(\mathbf{Q}^{\mathrm{LAG}}) = (0,0,0,0,\rho\phi)^T$. The corresponding HLLC flux vector consists of a single state:

$$\left(F^{\mathrm{LAG}}\right)^{\mathrm{HLLC}}_{i+1/2} = (-u^*, p^*, p^*u^*, 0, 0)_{i+1/2}, \tag{26}$$

where

$$u^*_{i+1/2} = \frac{u_i + u_{i+1}}{2} + \frac{p_i - p_{i+1}}{2a_{i+1/2}}, \tag{27a}$$

$$p^*_{i+1/2} = \frac{p_i + p_{i+1}}{2} + \frac{a_{i+1/2}}{2}(u_i - u_{i+1}), \tag{27b}$$

and where the acoustic impedance $a_{i+1/2}$ at the interface is approximated using the choice of Chalons et al. [6]:

$$a_{i+1/2} = \max(\rho_i c_i, \rho_{i+1} c_{i+1}). \tag{28}$$

The interfacial term of the topology equation is approximated at first order by

$$\int_{C_i} \partial_m u \mathrm{d}C_i \doteq \tau_i \left(u^*_{i+1/2} - u^*_{i-1/2}\right). \tag{29}$$

Summarizing, the update formula for the discretized acoustic system reads, making an explicit forward Euler time step:

$$\begin{aligned} \mathbf{Q}_i^{n+1-} = \mathbf{Q}_i^n &- \frac{\Delta t}{\rho_i^n \Delta x}\left(F^n_{i+1/2} - F^n_{i-1/2}\right) \\ &- \phi_i^n \frac{\Delta t}{\Delta x}\left(\mathscr{H}^n_{i+1/2} - \mathscr{H}^n_{i-1/2}\right), \end{aligned} \tag{30}$$

where

$$(\mathbf{Q}_i)^T = (\tau, u, E, \beta_1, \alpha_1)_i, \tag{31a}$$

$$\left(F^n_{i+1/2}\right)^T = (-u^*, p^*, p^*u^*, 0, 0)^n_{i+1/2}, \tag{31b}$$

$$\left(\mathscr{H}^n_{i+1/2}\right)^T = (0,0,0,0,u^*)^n_{i+1/2}. \tag{31c}$$

Transport system

The transport system is approximated by using a classical finite-volume upwind scheme as employed in Chalons et al. [6]. The scheme reads, making again an explicit forward Euler time step:

$$\begin{aligned} \upsilon_i^{n+1} = \upsilon_i^{n+1-} &- \frac{\Delta t}{\Delta x}\left(u^*_{i+1/2}\upsilon^{n+1-}_{i+1/2} - u^*_{i-1/2}\upsilon^{n+1-}_{i-1/2}\right) \\ &+ \frac{\Delta t}{\Delta x}\upsilon_i^{n+1-}\left(u^*_{i+1/2} - u^*_{i-1/2}\right), \end{aligned} \tag{32}$$

where $\upsilon \in \{\rho, \rho u, \rho E, \alpha_1\rho_1, \alpha_1\}$. The upwind value is used to approximate the interface value $\upsilon_{i+1/2}$:

$$\upsilon^{n+1-}_{i+1/2} = \begin{cases} \upsilon_i^{n+1-}, & \text{if} \quad u^*_{i+1/2} \geq 0, \\ \upsilon_{i+1}^{n+1-}, & \text{if} \quad u^*_{i+1/2} < 0. \end{cases} \tag{33}$$

Stability requirement

The time step in the explicit time integration method is obtained using the Courant numbers of both subsystems. The Courant numbers are given by

$$\mathscr{C}_a = \frac{\Delta t}{\Delta x}\max_i\left(\max(\tau_i^n, \tau_{i+1}^n)a_{i+1/2}\right), \tag{34}$$

for the acoustic subsystem, and by

$$\mathscr{C}_t = \frac{\Delta t}{\Delta x}\max_i\left(\left(u^*_{i-1/2}\right)^+ - \left(u^*_{i+1/2}\right)^-\right), \tag{35}$$

for the transport subsystem, where $b^{\pm} = (b \pm |b|)/2$. The time step is determined by the requirement that the Courant numbers need to be less than one. In the implementation, the most severe time step restriction is taken for both subsystems. Hence, the time step is selected with $\mathscr{C} = \max(\mathscr{C}_a, \mathscr{C}_t)$.

SHOCK TUBE TEST CASES

The robustness and accuracy of the novel Lagrange-projection-like numerical scheme is assessed. The considered test cases are shock tube problems in which a left fluid state and a right fluid state are separated by a membrane, see Figure 1.

FIGURE 1. A schematic view of a shock tube with two fluid states.

At the open ends of the shock tube transmissive boundary conditions are imposed. The numerical method is evaluated in the following three two-phase shock-tube problems: a translating interface problem, a pressure jump problem and a mixture problem. All tests are performed in one dimension, with first order accuracy in space.

Translating two-phase interface

In this first test case, also used by e.g. [4], a dense gas pushes, at constant velocity and pressure, a much less dense gas rightwards. The interface is located at the middle of the shock tube ($X = 0.5$). This test case is assessed to investigate the behavior of the scheme at a contact discontinuity.

	ρ	u	p	β_1	α_1
Left state	1000	1.0	1.0	1.0	1.0
Right state	1.0	1.0	1.0	0.0	0.0

TABLE 1. Initial values pressure jump problem.

The initial conditions are given in Table 2. The thermodynamic constants are $\gamma_1 = 1.4$, $\pi_1 = 0.0$, $\gamma_2 = 1.6$, $\pi_2 = 0.0$. The results are obtained at time $t = 0.1$ s with $N = 400$ cells for the Courant number $\mathscr{C} = 0.95$. The distributions of the primitive variables are visualized in the Figures 2-5.

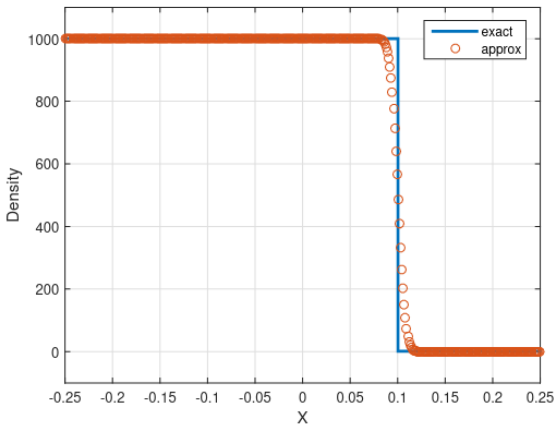

FIGURE 2. Test 1 - Density distribution along tube at $t = 0.1$ s.

The contact discontinuity is well retrieved with the proposed method. The location of two-phase interface for the mass fraction, see Figure 5, is a little bit off, similar as in [4]. Furthermore, no oscillations and no over- and undershoots are visible.

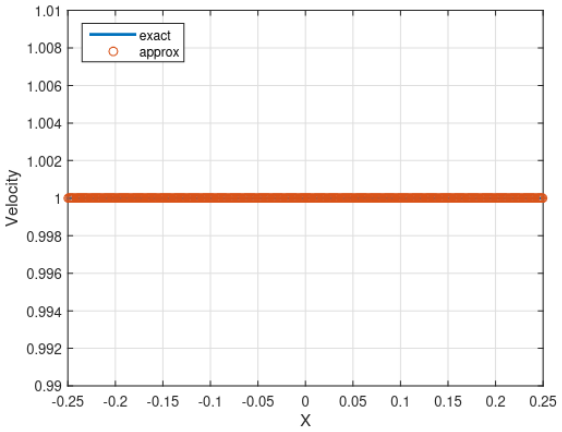

FIGURE 3. Test 1 - Velocity distribution along tube at $t = 0.1$ s.

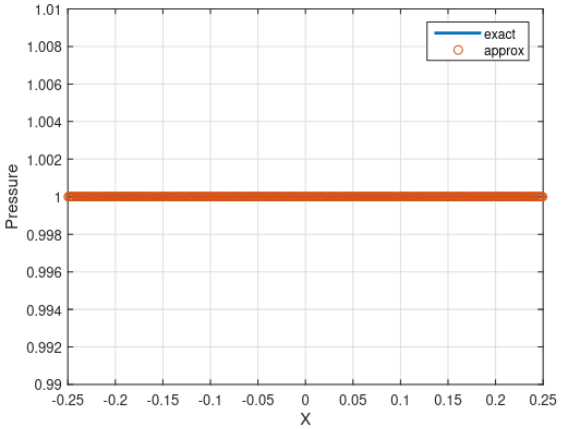

FIGURE 4. Test 1 - Pressure distribution along tube at $t = 0.1$ s.

A pressure jump problem

In this test case, proposed by Barberon et al. [9] and used in e.g. [5], a shock tube is filled with two gases at different density. The pressures at both sides are slightly different. The interface is located at $X = 0.5$ m. Due to the pressure difference, a shock wave will propagate rightwards.

The initial conditions are given in Table 2. The thermodynamic constants are $\gamma_1 = 1.4$, $\pi_1 = 0.0$, $\gamma_2 = 1.1$, $\pi_2 = 0.0$. The dimensions of the quantities ρ, u, p and π are kg m^{-3}, m s^{-1} and Pa, respectively. The results are obtained at time $t = 1.0$ ms with

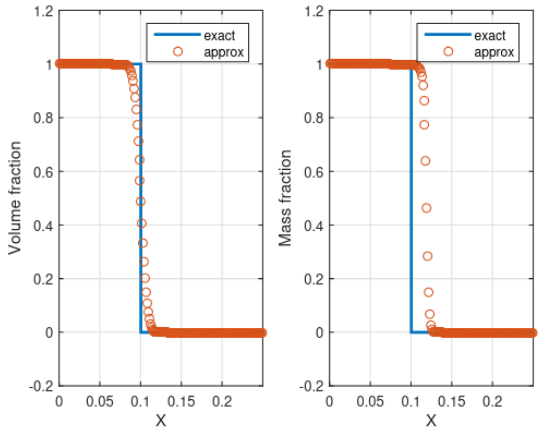

FIGURE 5. Test 1 - Volume fraction (left) and mass fraction (right) distribution along tube at $t = 0.1$ s.

	ρ	u	p	β_1	α_1
Left state	10	50.0	1.1×10^5	1.0	1.0
Right state	1.0	50.0	1.0×10^5	0.0	0.0

TABLE 2. Initial values pressure jump problem.

$N = 400$ cells for $\mathscr{C} = 0.95$. The distributions of the primitive variables are visualized in the Figures 6-9.

The location of the shock wave is satisfactorily retrieved with the proposed method. Furthermore, no oscillations and no over- and undershoots are visible.

Water-air mixture problem

In this shock tube test we consider a water-air mixture problem. This test case has been considered by Murrone and Guillard [3] and by Kreeft and Koren [4]. In contrast to the previous test cases, the shock tube is now filled with a mixture of water and air ($0 < \beta_1, \alpha_1 < 1$). Both mixture states are initially at rest. The pressure ratio is 10^4.

The initial conditions are given in Table 3. The thermodynamic constants for the SG EOS are $\gamma_1 = 1.4$, $\pi_1 = 0.0$, $\gamma_2 = 4.4$, $\pi_2 = 6.0 \times 10^8$. Again, the dimensions of the quantities ρ, u, p and π are kg m^{-3}, m s^{-1} and Pa, respectively. Numerical results are obtained at time $t = 200$ μs with $N = 400$ cells with $\mathscr{C} = 0.95$. The results are visualized in Figures 10-13.

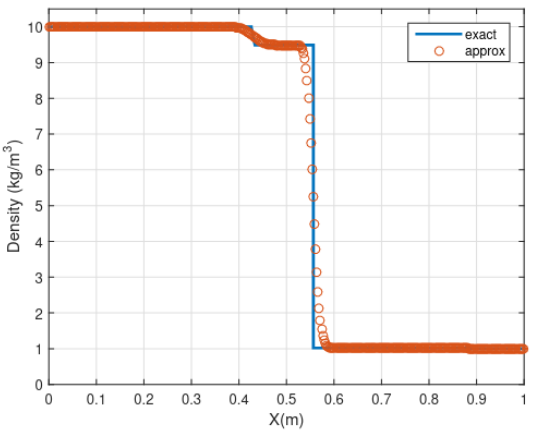

FIGURE 6. Test 2 - Density distribution along tube at $t = 1$ ms.

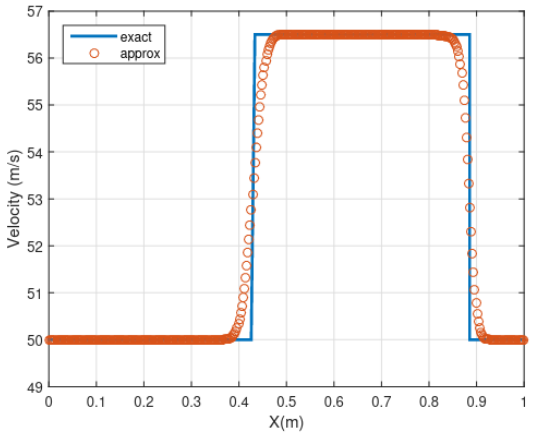

FIGURE 7. Test 2 - Velocity distribution along tube at $t = 1$ ms.

	ρ	u	p	β_1	α_1
Fluid 1	525	0.0	10^9	0.0476	0.5
Fluid 2	525	0.0	10^5	0.9524	0.5

TABLE 3. Initial values water-air mixture problem.

The numerical results are compared with numerical solutions from [3]. The distributions are in perfect agreement with the reference solutions. The volume fraction distribution

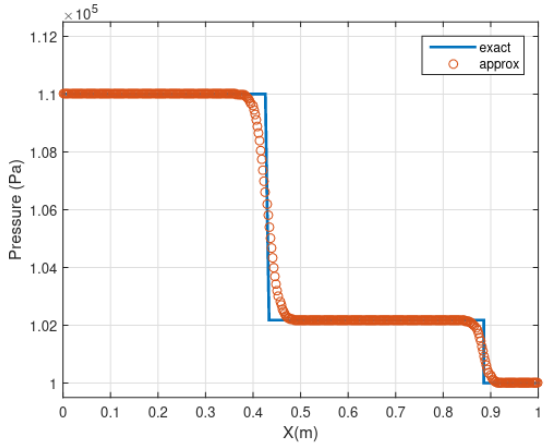

FIGURE 8. Test 2 - Pressure distribution along tube at $t = 1$ ms.

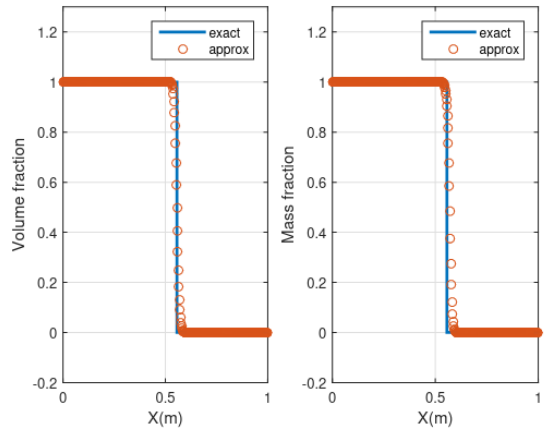

FIGURE 9. Test 2 - Volume fraction (left) and mass fraction (right) distribution along tube at $t = 1$ ms.

of [3], in Figure 13, shows on the right side a little lower value compared with the proposed method. Again, no oscillations and no over- and undershoots are visible. This test case indicates that the numerical scheme can deal with mixture problems.

CONCLUSION

A novel splitting-based Lagrange-projection-like numerical scheme is presented for the Kapila five-equation model in which pressure and velocity equilibrium between the phases is

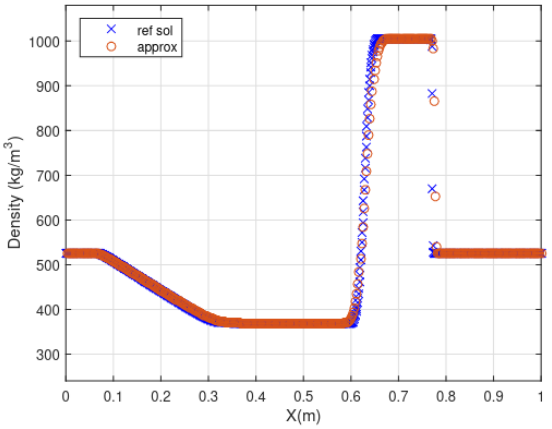

FIGURE 10. Test 3 - Density distribution along tube at $t = 200$ μs.

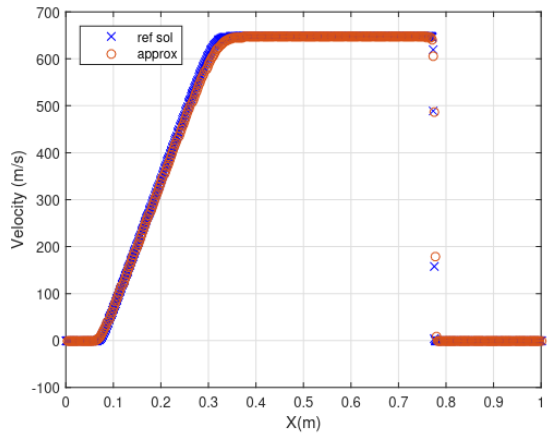

FIGURE 11. Test 3 - Velocity distribution along tube at $t = 200$ μs.

assumed. The model is decomposed into an acoustic and a transport part. The acoustic part is cast into Lagrangian formulation and is solved using an HLLC-type scheme. The transport subsystem is solved using a classical upwind scheme.

The assessed shock tube test cases show that the obtained numerical results are in good agreement with reference results. Current work concerns the development of the numerical scheme for low-Mach number cases.

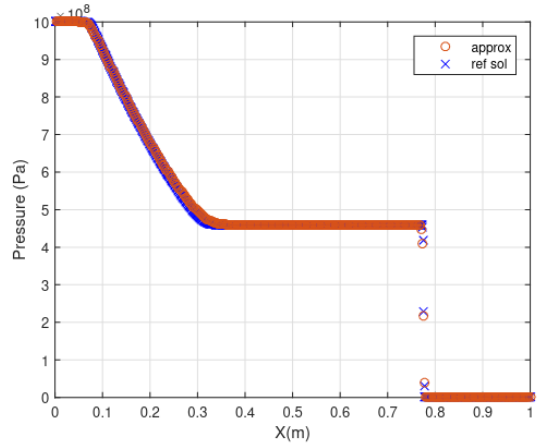

FIGURE 12. Test 3 - Pressure distribution along tube at $t = 200\ \mu$s.

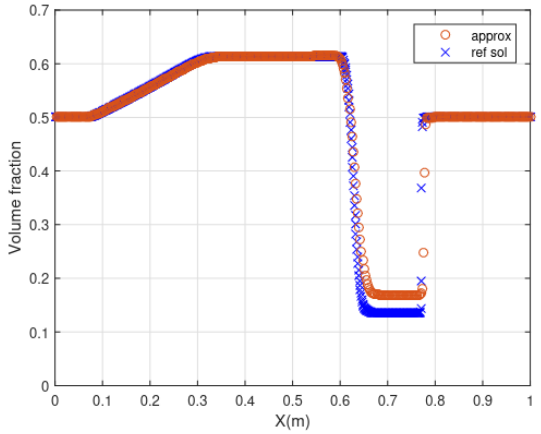

FIGURE 13. Test 3 - Volume fraction distribution along tube at $t = 200\ \mu$s.

ACKNOWLEDGMENT

Thanks go to Arris Tijsseling for pointing us at the PVP conference.

REFERENCES

[1] Kapila A.K., Menikoff R., Bdzil J.B., Son S.F., Stewart DS. Two-phase modeling of deflagration-to-detonation transition in granular materials: reduced equations. Phys Fluids, 13, 3002-3025 (2001).

[2] Baer M.R., Nunziato J.W., A two-phase mixture theory for the deflagration-to-detonation transition (ddt) in reactive granular materials. Int J Multiphase Flow 12, 861-889 (1986).

[3] Murrone A., Guillard H., A five equation reduced model for compressible two phase flow problems, J Comput Phys 202, 664-698 (2005).

[4] Kreeft J.J., Koren B., A new formulation of Kapila's five-equation model for compressible two-fluid flow, and its numerical treatment, J Comput Phys, 229, 6220-6242 (2010).

[5] Daude F., Galon P., Gao Z., Blaud E. Numerical experiments using a HLLC-type scheme with ALE formulation for compressible two-phase flows five-equation models with phase transition, Comput Fluids 94, 112-138, (2014).

[6] Chalons C., Girardin M., Kokh S., An all-regime Lagrange-Projection like scheme for the gas dynamics equations on unstructured meshes. Hal 01007622v2 (2014).

[7] Wood, A.B., A textbook of sound, London: G. Bell and Sons Ltd (1930).

[8] Toro E.F., Spruce M., Speares W., Restoration of the contact surface in the HLL-Riemann solver. Shock Waves 4, 25-34 (1994).

[9] Barberon T., Helluy P., Rouy S.. Practical computation of axisymmetrical multifluid flows. Int J Finite Volumes 1, 1-36 (2004).

[10] Harten A., Lax P.D., Van Leer B., On Upstream Differencing and Godunov-Type Schemes for Hyperbolic Conservation Laws. SIAM Review 25, 35-61 (1983).

[11] Saurel R., Petitpas F., Abgrall R., Modelling phase transition in metastable liquids: application to cavitating and flashing flows. J Fluid Mech, 607, 313-350 (2008).